
RiemannFormer: A Framework for Attention in Curved Spaces

Zhongping Ji

jzp@hdu.edu.cn
Hangzhou Dianzi University

ABSTRACT

The inherent permutation invariance of standard self-attention stems from its implicit assumption of a flat Euclidean geometry, where all spatial positions possess exchange symmetry. To fundamentally break this symmetry and endow the model with intrinsic geometric selectivity, we propose reframing attention as interactions on a curved Attention Manifold. In this framework, queries and keys are treated as vectors within the manifold’s intrinsic geometry, residing in the tangent bundle. Here, a Riemannian metric governs the local geometry, defining both the connection for parallel transport and the local inner product for similarity computation. In stark contrast, we propose that value vectors are sections of a separate, trivial vector bundle, decoupling the geometric alignment of Q/K from the feature aggregation of V .

Our primary contribution is a novel, first-principles construction of this parallel transport using Lie group theory, where for 2D data, we derive a positional encoding from the exceptional isomorphism $\mathfrak{so}(4) \cong \mathfrak{su}(2) \oplus \mathfrak{su}(2)$. This allows us to factorize 4D rotations into two commuting isoclinic rotations aligned with the spatial dimensions. Furthermore, we introduce a Riemannian Attention Mechanism that strategically decouples metric scaling from the softmax normalization. Drawing inspiration from the physical principle that matter determines the geometry of space, we devise a dynamic metric scaling governed by the token embeddings themselves. This allows semantic content to locally modulate the geometry of the manifold, naturally inducing a content-aware focus that adaptively highlights salient regions. Experimental results demonstrate that our modules deliver significant performance improvements over strong baselines, and further evaluations on visual and large language models are underway.

Keywords Transformer · Self-Attention · Curved Space · Tangent Bundle · Fiber Bundle · Parallel Transport

1 Introduction

The transformer architecture, introduced in the seminal paper by Vaswani et al. [1], has revolutionized the field of natural language processing (NLP) and extended its impact to computer vision, audio processing, and other domains. The iterative application of transformer blocks allows tokens to progressively capture higher-level semantic concepts, making the architecture highly effective for tasks requiring contextual understanding.

The transformer block operates on a sequence of tokens, each represented as a vector of fixed dimensionality d_{model} . For a sequence of N tokens, the input to the block is a matrix $X \in \mathbb{R}^{N \times d_{\text{model}}}$, where each row corresponds to a token’s embedding. The transformer block processes this matrix through its core component, Multi-Head Self-Attention (MHSA). The MHSA mechanism is the cornerstone of the transformer, enabling it to aggregate information globally across all tokens in the input sequence. Unlike convolutional neural networks (CNNs), which rely on local receptive fields, or recurrent neural networks (RNNs), which process sequences sequentially, self-attention allows each token to attend to all other tokens simultaneously, capturing long-range dependencies efficiently. Specifically, the attention mechanism computes a score for each pair of tokens by taking the dot product of their query and key vectors, scaled

to prevent large values that could destabilize training: $\text{Attention}(\mathbf{Q}, \mathbf{K}, \mathbf{V}) = \text{softmax}\left(\frac{\mathbf{Q}\mathbf{K}^\top}{\sqrt{d_k}}\right)\mathbf{V}$. The dot product $\mathbf{Q}\mathbf{K}^\top \in \mathbb{R}^{N \times N}$ measures the similarity between the query vector of one token and the key vectors of all tokens, producing an attention score matrix. The softmax function normalizes the scores across the key dimension, converting them into weights that sum to 1 for each query. This ensures that the attention mechanism focuses on the most relevant tokens. The resulting weights are used to compute a weighted sum of the value vectors, producing a new representation for each token that incorporates information from all other tokens. The output of the attention mechanism is a matrix, where each row is a context-aware representation of the corresponding input token. Moreover, the attention mechanism is permutation-equivariant, meaning the output does not depend on the order of the input tokens unless positional information is explicitly added.

Since the self-attention mechanism is permutation-equivariant, it does not inherently capture the order of tokens. To address this, transformers incorporate positional encodings or positional embeddings, which are added to the input token embeddings before processing. Below, we provide a brief overview of positional encodings in transformer. Positional encodings are indispensable in transformer models, embedding sequential order into permutation-equivariant self-attention mechanisms to enable token position modeling in tasks like natural language processing and vision. The seminal sinusoidal positional encodings, introduced by Vaswani et al. [1], remain prevalent due to their deterministic nature and ability to generalize across arbitrary sequence lengths. In contrast, learned positional encodings, as used in BERT [2], optimize trainable embeddings for task-specific patterns but falter in extrapolating to longer sequences. Relative positional encodings, adopted in Transformer-XL [3], T5 [4], and TUPE [5], model token distance relationships, enhancing generalization for long-context tasks. Rotary Positional Embeddings (RoPE) efficiently encode relative positions by applying rotation matrices to query and key vectors [6], with extensions like xPos [7] incorporating dynamic scaling for stable long-sequence training. Recent innovations include ALiBi [8], which simplifies computation by introducing attention biases based on token distances. Prior methods like absolute and relative positional encoding are static post-training. Zheng et al. propose Data-Adaptive Positional Encoding (DAPE), which adjusts dynamically based on input context and learned priors [9]. In addition, Golovneva et al. introduced Contextual Position Encoding (CoPE) [10], a novel position encoding method that conditions positions on context by selectively incrementing positions based on model-determined tokens. Although methods like ALiBi and adaptive PEs reduce complexity, they may introduce instability in extremely long sequences, and their generalization across diverse domains remains underexplored.

Since its adaptation to visual tasks with the Vision Transformer (ViT) [11], the transformer has demonstrated exceptional performance across a wide range of applications, from high-level tasks like classification [12] and detection [13] to low-level tasks such as super-resolution and generation. ViTs process images by dividing them into fixed-size patches, which are then treated as tokens similar to words in a sentence. These patches are embedded and fed into a transformer encoder, which leverages self-attention mechanisms to capture global relationships within the image. This approach allows ViTs to learn complex patterns and dependencies across the entire image, leading to impressive performance on various benchmarks. Positional encoding is a crucial component in the application of transformers to visual tasks, enabling the model to retain spatial information about the input image. Unlike natural language processing tasks where the sequence of words carries inherent positional information, images are divided into patches that lack such sequential context. Positional encodings allow the model to account for the order and arrangement of the patches, which is essential for understanding the spatial relationships and structure within the image. The original ViT model uses fixed positional encodings, similar to those used in the original Transformer model for NLP tasks. In addition to learnable and relative positional encodings, alternative schemes have emerged. RoPE excels in language models, particularly in enhancing transformer length extrapolation, yet its potential in computer vision remains largely unexplored. Heo et al. analyzes RoPE’s application to ViT, demonstrating significant improvements in visual tasks like classification, detection and segmentation, with minimal computational overhead [14]. Chu et al. introduce conditional positional encoding for ViT, dynamically generated based on local input token context [15]. These approaches potentially provide a more flexible and scalable approach to positional encoding in ViTs.

Despite its strengths, positional encodings require further interpretation and improvement. The mechanistic role of positional information remains unclear, offering a promising direction for future research. To better elucidate the attention mechanism, we endeavor to investigate the deeper implications underlying positional encoding in this paper. In addition, transformers often benefit from being trained on massive datasets. Larger datasets allow transformers to learn more nuanced patterns and relationships in the data, leading to better accuracy and generalization. However, transformers often exhibit suboptimal performance when applied to small datasets. Through experimental analysis, we have found that the introduction of an explicit locality focusing mechanism significantly enhances the performance of transformer in visual tasks.

Motivation & Intuition. The inherent permutation invariance of standard self-attention stems from its implicit assumption of a flat Euclidean geometry. In such a homogeneous space, the metric structure is globally uniform ($\mathbf{M} = \mathbf{I}$), rendering all spatial positions geometrically indistinguishable and possessing a discrete translational

symmetry. To fundamentally break this symmetry without relying on ad-hoc additive encodings, we propose embedding token sequences into a non-flat Riemannian Manifold.

In this curved geometry, the symmetry is naturally broken by the intrinsic structure of the manifold. Crucially, this Riemannian framework offers a dual advantage: it not only encodes spatial relationships via curvature but also quantifies the intrinsic importance of each token via the metric scale. By allowing the local metric to vary, we transform the "flat" attention landscape into a dynamic topography where salient features create "gravity wells", thereby endowing the self-attention mechanism with a geometrically principled selectivity.

2 Methodology

Consider a sequence comprising N input tokens, with their embeddings represented as $\{\mathbf{x}_i\}_{i=1}^N$, where $\mathbf{x}_i \in \mathbb{R}^D$ denotes the D -dimensional embedding vector for the i -th token, devoid of positional information. In this paper, we adopt an alternative perspective: we posit the existence of a curved space \mathcal{M} wherein the encoding of a token sequence corresponds to identifying a sequence of points $\{\mathbf{p}_i\}$, or a grid of points $\{\mathbf{p}_{ij}\}$ for image data, etc.

2.1 Attention Manifold

We introduce the concept of the Attention Manifold, a novel framework for interpreting Transformer self-attention through non-Euclidean geometry. In this view, token positions are points on a manifold, and their feature embeddings are vectors in the corresponding tangent spaces. The manifold's geometry is defined by a Riemannian metric, which modulates local interactions and encodes semantic saliency, and a parallel transport operator, which ensures consistent comparisons between vectors at different positions. This geometric formulation provides a first-principles approach to designing attention mechanisms with strong, built-in inductive biases.

Our approach is motivated by a fundamental shift in perspective from an extrinsic to an intrinsic geometric viewpoint. From this standpoint, a manifold is not defined by the absolute coordinates of its points within some ambient space, but rather by the complete set of relationships and transformations that connect them. Consequently, our primary objective is not to parameterize the absolute locations of tokens. Instead, we focus entirely on the crucial task: to directly define a consistent and computationally tractable protocol for the transport of tangent vectors (the feature embeddings) between the tangent spaces at discrete points. In essence, what matters is not where the tokens are, but how their representations can be transformed into one another.

Formally, in differential geometry, the parallel transport of a vector field V along a parameterized curve $c(t)$ is governed by the condition that its covariant derivative along the curve is zero. In local coordinates, this translates to a system of differential equations:

$$\frac{dv^k}{dt} + \Gamma_{ij}^k \frac{dc^i}{dt} v^j = 0,$$

where $c(t)$ is the path between points, and Γ_{ij}^k are the connection coefficients (e.g., Christoffel symbols) that encode the manifold's curvature.

However, this formal definition presents a fundamental challenge for our discrete and non-parametric setting. We intentionally avoid the complexity and high cost of explicitly defining the manifold's embedding, the continuous paths $c(t)$ between tokens, or the connection coefficients Γ_{ij}^k . Consequently, this system of equations, while theoretically fundamental, is practically intractable within our framework as we lack the necessary components for its solution. This raises the central question: how can we define a consistent and computationally tractable parallel transport operator without recourse to the underlying continuous geometry? Specifically, the vectors \mathbf{q}_i and \mathbf{k}_i reside in the tangent spaces $T_{\mathbf{p}_i}\mathcal{M}$ at position \mathbf{p}_i . For instance, \mathbf{q}_m and \mathbf{k}_m both belong to the tangent space $T_{\mathbf{p}_m}\mathcal{M}$ at point \mathbf{p}_m , whereas \mathbf{q}_m and \mathbf{k}_n are situated in the tangent spaces at points \mathbf{p}_m and \mathbf{p}_n , respectively. The inner product in the tangent space $T_{\mathbf{p}_m}\mathcal{M}$ at point \mathbf{p}_m is defined as $\mathbf{x}_1^\top \mathbf{M}_m \mathbf{x}_2$, where \mathbf{M}_m is a Riemannian metric specifying the inner product structure at \mathbf{p}_m . Since \mathbf{k}_n does not belong to the tangent space at \mathbf{p}_m , it is not appropriate to directly perform inner products such as $\mathbf{q}_m^\top \mathbf{M}_m \mathbf{k}_n$. To address this, a transformation $\mathbf{f}_{n,m}(\mathbf{k}_n)$ is required to appropriately transport \mathbf{k}_n from the tangent space at \mathbf{p}_n to that at \mathbf{p}_m . Only after this transformation can a valid inner product be executed, given by $\mathbf{q}_m^\top \mathbf{M}_m \mathbf{f}_{n,m}(\mathbf{k}_n)$.

Let us now formalize the attention mechanism within our geometric framework. We consider a discrete sequence of points, $\{\mathbf{p}_i\}_{i=1}^N$, defined on the Attention Manifold \mathcal{M} . The collection of all tangent spaces on the manifold, $\{T_{\mathbf{p}}\mathcal{M}\}_{\mathbf{p} \in \mathcal{M}}$, forms a structure known as the Tangent Bundle, denoted $T\mathcal{M}$. We conceptualize the query and key representations as sections of this tangent bundle. The query and key vector fields, Q and K , therefore assign a

tangent vector $\mathbf{q}_i, \mathbf{k}_i \in T_{\mathbf{p}_i}\mathcal{M}$ to each point \mathbf{p}_i . These vectors live within the intrinsic, and potentially curved, geometry of the manifold. In stark contrast, the value representations are treated as sections of a Trivial Vector Bundle, $\mathcal{M} \times \mathbb{R}^{D_v}$. This construction places the value vectors $\{\mathbf{v}_i\}$ in a global, geometry-agnostic Euclidean space. This trivial bundle construction formally decouples the geometric interactions of queries and keys on the manifold from the value representations. A principal advantage of this decoupling is the architectural flexibility it affords: the dimensionality of the value vectors, D_v , is not required to match the dimensionality of the tangent spaces, D , where queries and keys reside. This allows for independent design choices, mirroring the flexibility found in standard Multi-Head Attention architectures. At each point $\mathbf{p}_i \in \mathcal{M}$, we sample a specific query and key vector $\mathbf{q}_i \in T_{\mathbf{p}_i}\mathcal{M}$ and $\mathbf{k}_i \in T_{\mathbf{p}_i}\mathcal{M}$ from their respective fields, where the tangent space has dimension D . The core of the attention mechanism is the interaction between a query vector \mathbf{q}_i at point \mathbf{p}_i and key vectors from all other points, $\{\mathbf{k}_j\}$. To perform a geometrically consistent comparison, each key vector \mathbf{k}_j is first transported from its native tangent space $T_{\mathbf{p}_j}\mathcal{M}$ to the query’s tangent space $T_{\mathbf{p}_i}\mathcal{M}$. The attention scores are then computed via the local inner product.

Finally, these scalar scores are normalized to form attention weights. These weights are then used to compute a weighted sum of the value vectors $\{\mathbf{v}_j\}$ in their common Euclidean space \mathbb{R}^{D_v} . This aggregation, which does not require parallel transport of the values, yields the updated representation at position \mathbf{p}_i , which itself is a vector in \mathbb{R}^{D_v} .

2.2 Parallel Transport

In Euclidean space, tangent spaces at various points are isomorphic via translation, enabling straightforward vector transfer. This identification stems from the flat, homogeneous nature of Euclidean geometry, allowing parallel vector movement without additional geometric considerations. On a Riemannian manifold, parallel transport moves vectors along curves, maintaining consistency with intrinsic geometry structure of the manifold during transfer between tangent spaces. To be more specific, the vectors \mathbf{q}_m and \mathbf{k}_n ($m \neq n$) are in tangent spaces at different positions \mathbf{p}_i respectively. Prior to performing the inner product, it is necessary to adapt the vectors to the same space. This can be accomplished, for instance, by applying a parallel transport, denoted as $\mathcal{P}_{n \rightarrow m}(\mathbf{k}_n)$, that transports \mathbf{k}_n into the tangent space at \mathbf{q}_m .

Preliminaries: The parallel transport of tangent vectors $\mathbf{v} \in T_{c(\alpha)}\mathcal{M}$ to the tangent space $T_{c(\beta)}\mathcal{M}$ along a curve $c(t) : [0, 1] \rightarrow \mathcal{M}$ is denoted by $\Gamma_{c[\alpha, \beta]}(\mathbf{v})$. Two fundamental properties can be leveraged:

1) $\Gamma_{c[\alpha, \beta]} : T_{c(\alpha)}\mathcal{M} \rightarrow T_{c(\beta)}\mathcal{M}$ is a linear map.

2) Consider a Riemannian manifold \mathcal{M} equipped with its associated Riemannian connection ∇ . Let V be a parallel vector field along a parameterized curve $c(t) : [0, 1] \rightarrow \mathcal{M}$. The vector field V maintains a constant magnitude along the curve c .

To summarize, parallel transport provides a way of moving tangent vectors along a curve using the affine connection, and this provides a linear isomorphism between the tangent spaces at the two ends of the curve. However, the isomorphism obtained in this way will in general depend on the choice of the curve. Furthermore, it must be noted that we lack knowledge of the positions of points, curves, and additional structures (such as explicitly defined connection). Consequently, how can we achieve the parallel transport of tangent vectors? In fact, our methodology does not involve the explicit positional embeddings. Instead, we appoint the points and the curves connecting them in the order of tokens and enable the model to learn the linear mappings between tangent spaces at different points. Through these linear mappings, we can perform valid inner product without involving specific positional information.

To formalize the geometric concepts of vector magnitude and the defining property of our parallel transport operator, we can express the squared norm of a tangent vector in both abstract and computational forms. A tangent vector, such as the key vector \mathbf{k}_n at position \mathbf{p}_n , is expressed in a local coordinate basis $\{\partial_i\}$ as a linear combination $\sum_i k_n^i \partial_i$, where $\{k_n^i\}$ are its components.

The squared norm of this vector is computed via the inner product defined by the metric tensor \mathbf{M}_n at that point. This relationship is articulated by the following equation:

$$\underbrace{\langle \sum_i k_n^i \partial_i, \sum_j k_n^j \partial_j \rangle_{\mathbf{p}_n}}_{\text{Abstract Inner Product}} = \underbrace{\mathbf{k}_n^\top \mathbf{M}_n \mathbf{k}_n}_{\text{Computational Form}} = \underbrace{\mathcal{P}_{n \rightarrow m}(\mathbf{k}_n)^\top \mathbf{M}_m \mathcal{P}_{n \rightarrow m}(\mathbf{k}_n)}_{\text{Isometry under Parallel Transport}}. \quad (1)$$

By the property of bilinearity, the inner product expands to $\sum_{i,j} k_n^i k_n^j \langle \partial_i, \partial_j \rangle_{\mathbf{p}_n}$. The components of the metric tensor \mathbf{M}_n are, by definition, the inner products of the basis vectors themselves: $(\mathbf{M}_n)_{ij} = \langle \partial_i, \partial_j \rangle_{\mathbf{p}_n}$. Substituting this definition directly yields the familiar quadratic form $\mathbf{k}_n^\top \mathbf{M}_n \mathbf{k}_n$, where \mathbf{k}_n is the column vector of components $\{k_n^i\}$. This term represents the squared magnitude of the vector \mathbf{k}_n according to the local geometry at \mathbf{p}_n .

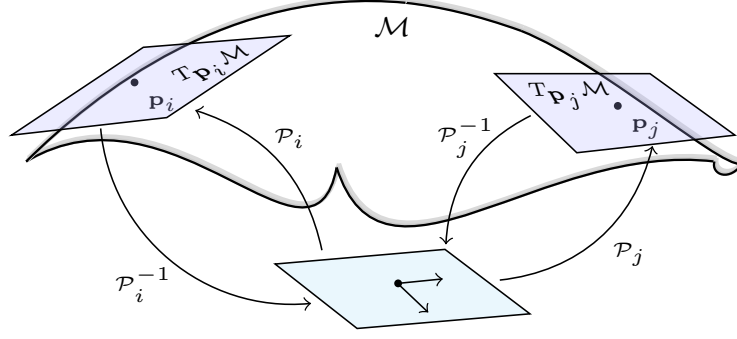


Figure 1: Maps between tangent spaces.

First, we introduce a common reference space \mathbb{R}^D , upon which the linear transformations between tangent spaces at various points are subsequently learned. As shown in Fig. (1), the linear transformation to be learned at point \mathbf{p}_i is denoted by $\mathcal{P}_i : \mathbb{R}^D \rightarrow T_{\mathbf{p}_i}\mathcal{M}$ and can be represented by a $D \times D$ matrix \mathbf{T}_i . In this study, we term the transformation \mathcal{P}_i^{-1} as tangent mapping or tangent aligning.

Building upon the foregoing analysis, we formally define the parallel transport operator, $\mathcal{P}_{n \rightarrow m}$, which transports a vector \mathbf{k}_n from the tangent space at position n to that at position m . This is achieved by composing the inverse transformation at the source with the forward transformation at the destination:

$$\mathcal{P}_{n \rightarrow m}(\mathbf{k}_n) = \mathcal{P}_m \circ \mathcal{P}_n^{-1}(\mathbf{k}_n) = \mathbf{T}_m \mathbf{T}_n^{-1} \mathbf{k}_n. \quad (2)$$

This formulation inherently satisfies the property of transitivity. A composition of transport operations from n to m and subsequently from m to l simplifies to a single direct transport from n to l . This is demonstrated by the algebraic cancellation of the intermediate operators, which confirms the robustness of our framework and a consistent geometric structure:

$$\begin{aligned} \mathcal{P}_{n \rightarrow m \rightarrow l}(\mathbf{k}_n) &= \mathcal{P}_l \circ \mathcal{P}_m^{-1} (\mathcal{P}_m \circ \mathcal{P}_n^{-1}(\mathbf{k}_n)) \\ &= \mathbf{T}_l \mathbf{T}_m^{-1} \mathbf{T}_m \mathbf{T}_n^{-1} \mathbf{k}_n \\ &= \mathbf{T}_l \mathbf{T}_n^{-1} \mathbf{k}_n \\ &= \mathcal{P}_{n \rightarrow l}(\mathbf{k}_n). \end{aligned} \quad (3)$$

Substituting Eq. (2) into Eq. (1), we obtain:

$$\mathbf{k}_n^\top \mathbf{M}_n \mathbf{k}_n = \mathbf{k}_n^\top (\mathbf{T}_n^{-1})^\top \mathbf{T}_m^\top \mathbf{M}_m \mathbf{T}_m \mathbf{T}_n^{-1} \mathbf{k}_n. \quad (4)$$

Given the arbitrariness of \mathbf{k}_n , it consequently follows that:

$$\mathbf{M}_n = (\mathbf{T}_n^{-1})^\top \mathbf{T}_m^\top \mathbf{M}_m \mathbf{T}_m \mathbf{T}_n^{-1}. \quad (5)$$

Then, simultaneously left-multiplying by matrix \mathbf{T}_n^\top and right-multiplying by matrix \mathbf{T}_n , we obtain:

$$\mathbf{T}_n^\top \mathbf{M}_n \mathbf{T}_n = \mathbf{T}_m^\top \mathbf{M}_m \mathbf{T}_m. \quad (6)$$

The above relationship of these matrices is what we must consider when predefining them. The Riemannian metric \mathbf{M}_i is a symmetric positive matrix. To facilitate the model to effectively learn the linear transformations \mathbf{T}_i , we first decompose them into two components, including scaling and length-preserving in \mathbb{R}^D : $\mathbf{T}_i = \mathbf{S}_i \mathbf{R}_i$. The introduction of scaling part \mathbf{S}_i is motivated by the characteristics of the curved space and the existence of Riemannian metric. The scaling part is represented by a symmetric positive matrix, and its simple form is a diagonal matrix or a scalar matrix $s\mathbf{I}$, where \mathbf{I} is the identity matrix. For instance, we set $\mathbf{S}_i = \mathbf{M}_i^{-\frac{1}{2}}$, then we have $\mathbf{T}_i = \mathbf{M}_i^{-\frac{1}{2}} \mathbf{R}_i$. \mathbf{R}_i is an orthogonal

matrix used for length-preserving, and a rotation is naturally a candidate. A rotation in D -dimensional Euclidean space is a linear transformation that preserves lengths of vectors, and it can be represented by an $D \times D$ orthogonal matrix in the special orthogonal group $\mathbf{SO}(D)$.

Given these definitions, it is straightforward to verify that Eq. (6) holds. Furthermore, the metric-induced inner product can be readily converted into the standard inner product as shown in the following formula, thereby simplifying its implementation.

$$\begin{aligned}
\langle \mathbf{q}_m, \mathcal{P}_{n \rightarrow m}(\mathbf{k}_n) \rangle_{\mathbf{M}_m} &= \mathbf{q}_m^\top \mathbf{M}_m \mathcal{P}_{n \rightarrow m}(\mathbf{k}_n) = \mathbf{q}_m^\top [\mathbf{M}_m \mathbf{T}_m \mathbf{T}_n^{-1}] \mathbf{k}_n \\
&= \mathbf{q}_m^\top [\mathbf{M}_m \mathbf{M}_m^{-\frac{1}{2}} \mathbf{R}_m \mathbf{T}_n^{-1}] \mathbf{k}_n \\
&= \mathbf{q}_m^\top [\mathbf{M}_m^{\frac{1}{2}} \mathbf{R}_m \mathbf{T}_n^{-1}] \mathbf{k}_n \\
&= \langle \mathbf{T}_m^{-1} \mathbf{q}_m, \mathbf{T}_n^{-1} \mathbf{k}_n \rangle_{\mathbf{I}}.
\end{aligned} \tag{7}$$

To reiterate, the central aim of our work is to empower the model to learn the intrinsic geometry of the Attention Manifold where sequence data reside. This geometry is fully characterized by the fundamental objects: the set of Riemannian metric tensors $\{\mathbf{M}_m\}$ that define local inner products and the transformations between tangent spaces. However, a fully general and learnable parameterization for these objects would be computationally intractable and parametrically prohibitive. Therefore, the core of our contribution lies in introducing a principled, parameter-efficient construction for these geometric structures, using predefined configurations derived from Lie group theory.

A Riemannian metric \mathbf{M}_m can be represented by a symmetric positive definite matrix, but for the sake of simplifying the problem, we preset it as a symmetric positive definite diagonal matrix:

$$\mathbf{M}_m = \text{diag}(s_m^{(1)}, s_m^{(2)}, \dots, s_m^{(D)}), \tag{8}$$

where $\langle \partial_i, \partial_i \rangle_{\mathbf{p}_m} = s_m^{(i)}$, the superscript (i) denotes the component index. To enhance computational efficiency and reduce parametric complexity, we may constrain the metric tensor \mathbf{M}_m to be a scalar matrix of the form $\mathbf{M}_m = s_m \mathbf{I}$, where $s_m > 0$. This choice is geometrically equivalent to inducing a **conformal deformation** on the standard Euclidean space \mathbb{R}^D . In our geometric framework, this matrix \mathbf{M}_m is not merely a scaling factor; it is interpreted as the metric tensor that defines the local geometry of the tangent space at position m . Its primary function is to modulate the inner product, thereby assigning a notion of **semantic importance or saliency** to the token at that position.

2.3 Riemannian Attention Mechanism

The standard self-attention mechanism implicitly assumes a uniform Euclidean metric ($\mathbf{M} = \mathbf{I}$), treating all positions as equally important a priori. By introducing a position-dependent or embedding-dependent metric \mathbf{M}_m , we allow the model to differentiate the intrinsic significance of tokens. A larger scalar s_m effectively amplifies the length of the query vector \mathbf{q}_m and, consequently, the magnitude of its computed attention scores to all other keys. Thus, s_m acts as a control knob for the token's influence: a higher value signifies greater semantic importance, causing its query to have a stronger impact on the overall attention distribution.

Given the Riemannian metric tensor \mathbf{M}_m at position m , the interaction between a query at m and a key at n is given by:

$$\mathbf{q}_m^\top \mathbf{M}_m \mathbf{T}_m \mathbf{T}_n^{-1} \mathbf{k}_n = \langle \mathbf{T}_m^{-1} \mathbf{q}_m, \mathbf{T}_n^{-1} \mathbf{k}_n \rangle.$$

A direct incorporation of this term into the standard Transformer self-attention yields:

$$\text{Attn} = \text{softmax} \left(\frac{\mathbf{Q}' \mathbf{K}'^\top}{\sqrt{d_k}} \right) \mathbf{V},$$

where the i -th rows of \mathbf{Q}' and \mathbf{K}' are $\mathbf{T}_i^{-1} \mathbf{q}_i$ and $\mathbf{T}_i^{-1} \mathbf{k}_i$, respectively. Here, the transformation $\mathbf{T}_i = \mathbf{S}_i \mathbf{R}_i$ encapsulates both scaling and rotation. A primary motivation for introducing the scaling factor s_i is to differentiate the intrinsic importance of different positions. However, the normalization property of the standard softmax function ($\sum p_i = 1$) tends to counteract or "swallow" this scalar modulation, potentially diminishing its intended effect.

To address this, we propose the Riemannian Attention (RieAttn) mechanism. Instead of discarding softmax for unbounded alternatives like ReLU or Sigmoid, we retain the probabilistic interpretation of attention but decouple the metric scaling from the normalization step. We apply the rotational component $\mathbf{R}[\cdot]$ inside the softmax to determine directional alignment, while applying the metric scaling \mathbf{S} outside the softmax as a gating term:

$$\text{RieAttn} = \left(\mathbf{S} \odot \text{softmax} \left(\frac{\mathbf{R}[\mathbf{Q}] \mathbf{R}[\mathbf{K}]^\top}{\sqrt{d_k}} \right) \right) \mathbf{V} = \left(\mathbf{L} \mathbf{L}^\top \odot \text{softmax} \left(\frac{\mathbf{R}[\mathbf{Q}] \mathbf{R}[\mathbf{K}]^\top}{\sqrt{d_k}} \right) \right) \mathbf{V}. \quad (9)$$

Here, $\mathbf{R}[\cdot]$ denotes the application of the rotation \mathbf{R}_i to the i -th row vectors. $\mathbf{L} = [s_1, s_2, \dots, s_N]^\top \in \mathbb{R}^N$ is the scale vector collecting scaling factors for all positions. Since we model the Riemannian metric as a conformal deformation, the scalar modulation for the interaction between any two positions naturally corresponds to the product of their respective scaling factors. Consequently, the global modulation matrix \mathbf{S} emerges as the outer product $\mathbf{L} \mathbf{L}^\top$, ensuring a geometrically consistent and symmetric interaction structure.

We explore two distinct strategies for determining the scale vector \mathbf{L} :

1) Static Metric (Position-Dependent): The scaling factor is determined solely by the spatial location of the token. For 2D image data, this allows the model to learn a fixed "saliency map" of the image grid.

2) Dynamic Metric (Matter-Dependent): Motivated by the general relativistic principle that matter determines the geometry of spacetime, we propose that the metric at a specific location should be determined by its content (embedding) rather than just its coordinates.

For the dynamic setting, we model the scale vector as a function of the input embeddings: $\mathbf{L} = \mathbf{g}(\text{Proj}(\mathbf{X}))$. The projection $\text{Proj}(\mathbf{X}) = \mathbf{X} \mathbf{U}$, with learnable axes $\mathbf{U} \in \mathbb{R}^{D \times n_h}$ for each of the n_h attention heads, effectively distills the content of each token into a lower-dimensional "mass" representation. The modulation function \mathbf{g} then maps this "mass" to a scaling factor that determines the local curvature of the Attention Manifold, implementing the principle that matter curves space. This mechanism offers significant interpretability: in NLP, it allows the manifold to contract around low-semantic function words, naturally dampening their influence; in Vision, it acts as an implicit saliency filter, amplifying the metric scale of foreground objects while suppressing the background. While \mathbf{g} can be standard activation functions like Sigmoid or ReLU, we empirically find the following formulation effective:

$$\mathbf{L} = \mathbf{g}(\text{Proj}(\mathbf{X})) = \sqrt{\alpha} \exp(\mathbf{X} \mathbf{U}), \quad (10)$$

where α can be a learnable scalar and $\exp(\cdot)$ is applied element-wise. Consequently, for a single attention head, the scaling matrix \mathbf{S} becomes:

$$\mathbf{S} = \alpha \mathbf{L} \mathbf{L}^\top = \alpha \begin{bmatrix} s_1^2 & s_1 s_2 & \cdots & s_1 s_N \\ s_2 s_1 & s_2^2 & \cdots & s_2 s_N \\ \vdots & \vdots & \ddots & \vdots \\ s_N s_1 & s_N s_2 & \cdots & s_N^2 \end{bmatrix} = \alpha \exp \left(\begin{bmatrix} 2t_1 & t_1 + t_2 & \cdots & t_1 + t_N \\ t_2 + t_1 & 2t_2 & \cdots & t_2 + t_N \\ \vdots & \vdots & \ddots & \vdots \\ t_N + t_1 & t_N + t_2 & \cdots & 2t_N \end{bmatrix} \right),$$

where $t_i = \mathbf{X}_i \mathbf{U}$. Additionally, we can employ a more expressive Multilayer Perceptron (MLP) for the projection, defined as $\mathbf{L} = \mathbf{g}(\text{MLP}(\mathbf{X}))$. For instance, $s_i = \mathbf{g}(\text{ReLU}(\mathbf{x}_i \mathbf{W}_1) \mathbf{W}_2)$, where $\mathbf{W}_1 \in \mathbb{R}^{D \times d_h}$ and $\mathbf{W}_2 \in \mathbb{R}^{d_h \times n_h}$, with d_h representing the hidden dimension. This dynamic approach allows the attention mechanism to adaptively emphasize or suppress regions based on their semantic content, providing a robust inductive bias for semantic or visual understanding.

2.4 A Principled Decomposition of High-Dimensional Rotations

A rotation in \mathbb{R}^D can be represented by a $D \times D$ matrix in the special orthogonal group $\mathbf{SO}(D)$. It is well known that an element of $\mathbf{SO}(D)$ can be generated from the exponential of a skew-symmetric matrix X , denoted as $\exp(X)$. Specifically, the orthogonal Lie algebra $\mathfrak{so}(D = 2k)$:

$$\{X \mid X^\top + X = 0\}$$

yields D -dimensional special orthogonal matrices via the exponential map: $\exp(X) \in \mathbf{SO}(D)$.

For position i , we predefine the linear transformation as,

$$\mathbf{T}_i = \mathbf{M}_i^{-\frac{1}{2}} \exp(iX). \quad (11)$$

Subsequently, we obtain,

$$\begin{aligned} \mathbf{T}_m \mathbf{T}_n^{-1} &= \mathbf{M}_m^{-\frac{1}{2}} \exp(mX) \exp(-nX) \mathbf{M}_n^{\frac{1}{2}} \\ &= \mathbf{M}_m^{-\frac{1}{2}} \exp((m-n)X) \mathbf{M}_n^{\frac{1}{2}}, \end{aligned} \quad (12)$$

and

$$\langle \mathbf{q}_m, \mathcal{P}_{n \rightarrow m}(\mathbf{k}_n) \rangle_{\mathbf{M}_m} = \mathbf{q}_m^\top [\mathbf{M}_m \mathbf{T}_m \mathbf{T}_n^{-1}] \mathbf{k}_n = \langle \mathbf{T}_m^{-1} \mathbf{q}_m, \mathbf{T}_n^{-1} \mathbf{k}_n \rangle_{\mathbf{I}}. \quad (13)$$

It is worth noting that antisymmetric matrices possess $D(D-1)/2$ independent elements, thereby introducing a substantial number of learnable parameters. To reduce the number of learnable parameters and mitigate algorithmic complexity, we may alternatively learn subgroups of the orthogonal matrix group $\mathbf{SO}(D)$, such as Maximal Torus $(S^1)^k$, or subspaces of the orthogonal Lie algebra, such as Cartan subalgebras.

We uniformly designate the encoding scheme herein as **Parallel Transport of Embeddings (PaTE)**. When emphasizing a specific subspace, such as $\mathbf{SO}(4)$, it is denoted as PaTE- $\mathbf{SO}(4)$.

2.4.1 Decomposition into Commuting $\mathbf{SO}(2)$ Subgroups

The Lie algebra $\mathfrak{so}(2k)$ contains a subspace that is the direct sum of k copies of $\mathfrak{so}(2)$:

$$\mathfrak{h} = \bigoplus_{i=1}^k \mathfrak{so}(2)^{(i)} \subset \mathfrak{so}(2k).$$

This subspace serves as the Cartan subalgebra \mathfrak{h} , for which we can construct a basis consisting of k matrices $\{H_1, H_2, \dots, H_k\}$. Each basis matrix H_i is built using the 2×2 antisymmetric matrix J , which generates infinitesimal rotations in two dimensions:

$$J = \begin{bmatrix} 0 & -1 \\ 1 & 0 \end{bmatrix}.$$

Each H_i is a $2k \times 2k$ block-diagonal matrix, divided into k blocks of size 2×2 . All blocks are zero except the i -th diagonal block, which is J :

$$H_1 = \begin{bmatrix} J & 0 & \dots & 0 \\ 0 & 0 & \dots & 0 \\ \vdots & \vdots & \ddots & \vdots \\ 0 & 0 & \dots & 0 \end{bmatrix}, \quad H_2 = \begin{bmatrix} 0 & 0 & \dots & 0 \\ 0 & J & \dots & 0 \\ \vdots & \vdots & \ddots & \vdots \\ 0 & 0 & \dots & 0 \end{bmatrix}, \quad \dots, \quad H_k = \begin{bmatrix} 0 & 0 & \dots & 0 \\ 0 & 0 & \dots & 0 \\ \vdots & \vdots & \ddots & \vdots \\ 0 & 0 & \dots & J \end{bmatrix}.$$

Any element H within \mathfrak{h} can be expressed as:

$$H = \sum_{i=1}^k \theta_i H_i = \text{diag}(\theta_1 J, \theta_2 J, \dots, \theta_k J),$$

where $\theta_1, \theta_2, \dots, \theta_k$ are arbitrary real numbers, and $\text{diag}(B_1, B_2, \dots, B_n)$ denotes the block diagonal matrix with each B_i serving as a diagonal block. The matrix H represents simultaneous infinitesimal rotations on k orthogonal planes, with the "angular velocity" on each plane being θ_i .

From the perspective of Lie group theory, the exponential map $\exp(H)$ lies within the subgroup $\mathbf{SO}(2) \times \dots \times \mathbf{SO}(2) \subset \mathbf{SO}(2k)$. This subgroup consists of block-diagonal matrices, where each of the k blocks is an element of $\mathbf{SO}(2)$. Specifically, the exponential of H is

$$\exp(H) = \exp\left(\sum_{i=1}^k \theta_i H_i\right) = \text{diag}(\exp(\theta_1 J), \exp(\theta_2 J), \dots, \exp(\theta_k J)),$$

where a diagonal block $\exp(\theta_i J)$ is a 2×2 rotation matrix,

$$\exp(\theta_i J) = \cos(\theta_i)I + \sin(\theta_i)J = \begin{bmatrix} \cos(\theta_i) & -\sin(\theta_i) \\ \sin(\theta_i) & \cos(\theta_i) \end{bmatrix}.$$

The interaction between two positions m and n can be represented as

$$\begin{aligned} \exp(m\theta J) \exp(n\theta J)^{-1} &= \exp((m-n)\theta J) \\ &= \cos((m-n)\theta)I + \sin((m-n)\theta)J \\ &= \begin{bmatrix} \cos((m-n)\theta) & -\sin((m-n)\theta) \\ \sin((m-n)\theta) & \cos((m-n)\theta) \end{bmatrix}. \end{aligned}$$

In fact, for any real antisymmetric matrix X , there exists an orthogonal matrix Q such that $X = QHQ^\top$, where H is an element in the Cartan subalgebra \mathfrak{h} of $\mathfrak{so}(2k)$, and thus $\exp(X) = Q \exp(H) Q^\top$. Here, the rotation in the 2D subspace corresponds to setting $Q = I$, which simplifies the scenario but also limits its capacity for interactions across spatial dimensions. It is also worth noting that, under the aforementioned configuration, the proposed approach reduces to a conventional RoPE when setting the metric as $\mathbf{M}_i = \mathbf{I}$, thereby indicating that RoPE can be viewed as a special case of our framework.

To enhance interactions across more dimensions, one may consider rotational transformations within higher-dimensional subspaces.

2.4.2 SO(3) Subgroups

We can consider rotational transformations within 3-dimensional subspaces. We assume here that D is a multiple of 3, i.e., $D = 3k$.

First, we define the 3×3 unit antisymmetric matrix K corresponding to a unit rotation axis:

$$K = \begin{bmatrix} 0 & -c & b \\ c & 0 & -a \\ -b & a & 0 \end{bmatrix},$$

where $a^2 + b^2 + c^2 = 1$, i.e., $\mathbf{v} = [a, b, c]^\top$ is a unit vector representing the rotation axis. For a real number θ , the exponential of the antisymmetric matrix θK is:

$$\exp(\theta K) = I + \sin(\theta)K + (1 - \cos(\theta))K^2.$$

This is the classic Rodrigues' rotation formula, which gives a closed-form exponential map from the Lie algebra $\mathfrak{so}(3)$ to the Lie group $\mathbf{SO}(3)$, transforming an antisymmetric matrix encoding the rotation axis and angle into its corresponding rotation matrix.

Incorporating positional information:

$$\exp(m\theta K) = I + \sin(m\theta)K + (1 - \cos(m\theta))K^2.$$

Likewise, the interaction between two positions m and n can be represented as

$$\begin{aligned} \exp(m\theta K) \exp(n\theta K)^{-1} &= \exp((m-n)\theta K) \\ &= I + \sin((m-n)\theta)K + (1 - \cos((m-n)\theta))K^2. \end{aligned}$$

2.4.3 The Isoclinic Decomposition of $\mathbf{SO}(4)$

It is well-established that rotations in the special orthogonal group $\mathbf{SO}(4)$ are generated via the exponential map from its Lie algebra, $\mathfrak{so}(4)$. Elements $X \in \mathfrak{so}(4)$ are 4×4 real skew-symmetric matrices of the form:

$$X = \begin{bmatrix} 0 & x_1 & x_2 & x_3 \\ -x_1 & 0 & x_4 & x_5 \\ -x_2 & -x_4 & 0 & x_6 \\ -x_3 & -x_5 & -x_6 & 0 \end{bmatrix}.$$

However, for an arbitrary X , the direct computation of its matrix exponential, $\exp(X)$, is often complex and lacks a concise closed-form expression analogous to that in 2D, such as $\exp(\theta J) = \cos(\theta)I + \sin(\theta)J$ where $J^2 = -I$. To devise a more efficient and insightful computational framework, it is imperative to investigate the intrinsic algebraic structure of $\mathfrak{so}(4)$.

The key insight lies in an exceptional property of the $\mathfrak{so}(4)$ Lie algebra: it is the unique semi-simple Lie algebra that decomposes into a direct sum of two ideals. Specifically, $\mathfrak{so}(4)$ is isomorphic to the direct sum of two $\mathfrak{su}(2)$ Lie algebras:

$$\mathfrak{so}(4) \cong \mathfrak{su}(2) \oplus \mathfrak{su}(2).$$

Given the isomorphism between $\mathfrak{su}(2)$ and the Lie algebra of 3D rotations, $\mathfrak{so}(3) \cong \mathfrak{su}(2)$, the above relation leads to a more intuitive isomorphism over the real field: $\mathfrak{so}(4) \cong \mathfrak{so}(3) \oplus \mathfrak{so}(3)$. This profound structural property implies that the algebra of 4D rotations can be perfectly deconstructed into a combination of two independent, familiar $\mathfrak{so}(3)$ algebras. This foundational decomposition provides the basis for simplifying the exponential map by decomposing $\mathfrak{so}(4)$ into a direct sum of two subalgebras.

To realize this decomposition, we define two special sets of basis vectors in the six-dimensional vector space of $\mathfrak{so}(4)$, denoted $\{A_1, A_2, A_3\}$ and $\{B_1, B_2, B_3\}$. These bases respectively span two three-dimensional subalgebras, $\mathfrak{h}_1 = \text{span}\{A_1, A_2, A_3\}$ and $\mathfrak{h}_2 = \text{span}\{B_1, B_2, B_3\}$. Since their union forms a complete basis for $\mathfrak{so}(4)$, any skew-symmetric matrix X can be uniquely decomposed as $X = A + B$, where $A = \sum a_i A_i \in \mathfrak{h}_1$ and $B = \sum b_j B_j \in \mathfrak{h}_2$. Thus, $\mathfrak{so}(4)$ is the direct sum of its subalgebras \mathfrak{h}_1 and \mathfrak{h}_2 , denoted $\mathfrak{so}(4) = \mathfrak{h}_1 \oplus \mathfrak{h}_2$.

The principal advantage of this decomposition is the simplification of the exponential map. As any element $A \in \mathfrak{h}_1$ commutes with any element $B \in \mathfrak{h}_2$, the exponential of their sum factors into a product of exponentials:

$$\exp(X) = \exp(A + B) = \exp(A) \exp(B).$$

This reduces the computation for a complex 4D rotation to that of two independent, quasi-3D rotations, each admitting an efficient, closed-form solution.

The standard bases for implementing the decomposition $\mathfrak{so}(4) = \mathfrak{h}_1 \oplus \mathfrak{h}_2$ are defined as follows. The basis $\{A_1, A_2, A_3\}$ for the subalgebra \mathfrak{h}_1 is:

$$A_1 = \begin{bmatrix} 0 & 0 & 0 & -1 \\ 0 & 0 & -1 & 0 \\ 0 & 1 & 0 & 0 \\ 1 & 0 & 0 & 0 \end{bmatrix}, \quad A_2 = \begin{bmatrix} 0 & 0 & 1 & 0 \\ 0 & 0 & 0 & -1 \\ -1 & 0 & 0 & 0 \\ 0 & 1 & 0 & 0 \end{bmatrix}, \quad A_3 = \begin{bmatrix} 0 & -1 & 0 & 0 \\ 1 & 0 & 0 & 0 \\ 0 & 0 & 0 & -1 \\ 0 & 0 & 1 & 0 \end{bmatrix}.$$

Any element in \mathfrak{h}_1 is a linear combination of these bases. Consider a normalized generator J_A defined by a unit vector (a_1, a_2, a_3) such that $a_1^2 + a_2^2 + a_3^2 = 1$:

$$J_A = \sum_{i=1}^3 a_i A_i = \begin{bmatrix} 0 & -a_3 & a_2 & -a_1 \\ a_3 & 0 & -a_1 & -a_2 \\ -a_2 & a_1 & 0 & -a_3 \\ a_1 & a_2 & a_3 & 0 \end{bmatrix}.$$

By construction, J_A satisfies $J_A^2 = -I$, where I is the identity matrix. Its algebraic behavior is therefore analogous to the imaginary unit i . Consequently, its matrix exponential, derived from the Taylor series expansion, assumes a form akin to Euler's formula:

$$\exp(\theta_1 J_A) = \cos(\theta_1)I + \sin(\theta_1)J_A.$$

Expanding this expression yields an explicit rotation matrix in $\mathbf{SO}(4)$:

$$\exp(\theta_1 J_A) = \begin{bmatrix} \cos(\theta_1) & -a_3 \sin(\theta_1) & a_2 \sin(\theta_1) & -a_1 \sin(\theta_1) \\ a_3 \sin(\theta_1) & \cos(\theta_1) & -a_1 \sin(\theta_1) & -a_2 \sin(\theta_1) \\ -a_2 \sin(\theta_1) & a_1 \sin(\theta_1) & \cos(\theta_1) & -a_3 \sin(\theta_1) \\ a_1 \sin(\theta_1) & a_2 \sin(\theta_1) & a_3 \sin(\theta_1) & \cos(\theta_1) \end{bmatrix},$$

where θ_1 represents the angle of rotation about an axis defined by the vector (a_1, a_2, a_3) .

In a completely analogous manner, we define the second basis $\{B_1, B_2, B_3\}$, which spans the commuting subalgebra \mathfrak{h}_2 :

$$B_1 = \begin{bmatrix} 0 & 0 & 0 & 1 \\ 0 & 0 & -1 & 0 \\ 0 & 1 & 0 & 0 \\ -1 & 0 & 0 & 0 \end{bmatrix}, \quad B_2 = \begin{bmatrix} 0 & 0 & 1 & 0 \\ 0 & 0 & 0 & 1 \\ -1 & 0 & 0 & 0 \\ 0 & -1 & 0 & 0 \end{bmatrix}, \quad B_3 = \begin{bmatrix} 0 & -1 & 0 & 0 \\ 1 & 0 & 0 & 0 \\ 0 & 0 & 0 & 1 \\ 0 & 0 & -1 & 0 \end{bmatrix}.$$

We construct a normalized generator J_B from a unit vector (b_1, b_2, b_3) :

$$J_B = \sum_{i=1}^3 b_i B_i = \begin{bmatrix} 0 & -b_3 & b_2 & b_1 \\ b_3 & 0 & -b_1 & b_2 \\ -b_2 & b_1 & 0 & b_3 \\ -b_1 & -b_2 & -b_3 & 0 \end{bmatrix},$$

where $b_1^2 + b_2^2 + b_3^2 = 1$. The basis $\{B_i\}$ shares the same algebraic properties as $\{A_i\}$, leading to $J_B^2 = -I$ and the identical form for its exponential map:

$$\exp(\theta_2 J_B) = \cos(\theta_2)I + \sin(\theta_2)J_B,$$

where θ_2 is another independent angle of rotation.

Rotations generated by $A \in \mathfrak{h}_1$, such as $\exp(A)$, are termed left-isoclinic rotations, while those generated by $B \in \mathfrak{h}_2$ are right-isoclinic rotations. Any rotation in 4D can be uniquely decomposed into the product of a left-isoclinic and a right-isoclinic rotation, which commute. This gives rise to the exponential property $\exp(A + B) = \exp(A)\exp(B)$ for $A \in \mathfrak{h}_1$, $B \in \mathfrak{h}_2$.

Extension to Block-Diagonal Rotations in $\mathbf{SO}(4k)$

The powerful decomposition of $\mathfrak{so}(4)$ provides a clear blueprint for constructing and parameterizing a significant subgroup of higher-dimensional rotations within $\mathbf{SO}(4k)$. We can generalize this framework by considering the Lie algebra of block-diagonal skew-symmetric matrices, which generates a corresponding block-diagonal subgroup of $\mathbf{SO}(4k)$.

Let us define a specific Lie subalgebra of $\mathfrak{so}(4k)$ as the direct sum of k copies of $\mathfrak{so}(4)$:

$$\mathfrak{g} = \bigoplus_{i=1}^k \mathfrak{so}(4)^{(i)} \subset \mathfrak{so}(4k).$$

An element $H \in \mathfrak{g}$ is a $4k \times 4k$ block-diagonal matrix, where each block is an element of $\mathfrak{so}(4)$:

$$H = \text{diag}(X_1, X_2, \dots, X_k),$$

with each $X_i \in \mathfrak{so}(4)$. The off-diagonal blocks are all zero matrices.

A fundamental property of the matrix exponential is that it preserves this block-diagonal structure. The exponential of H is simply the block-diagonal matrix of the individual matrix exponentials:

$$\exp(H) = \text{diag}(\exp(X_1), \exp(X_2), \dots, \exp(X_k))$$

Since the exponential map takes an element from the Lie algebra $\mathfrak{so}(4)$ to the Lie group $\mathbf{SO}(4)$, each block $\exp(X_i)$ is a rotation matrix in $\mathbf{SO}(4)$. Consequently, $\exp(H)$ is an element of $\mathbf{SO}(4k)$, and the set of all such matrices forms a Lie subgroup that is the direct product of k copies of $\mathbf{SO}(4)$, embedded within $\mathbf{SO}(4k)$.

We can now apply the isoclinic decomposition to each block X_i independently. For each $i \in \{1, \dots, k\}$, we decompose X_i into its left-isoclinic and right-isoclinic components:

$$X_i = A_i + B_i,$$

where $A_i \in \mathfrak{h}_1^{(i)}$ and $B_i \in \mathfrak{h}_2^{(i)}$. Here, $\mathfrak{h}_1^{(i)}$ and $\mathfrak{h}_2^{(i)}$ are the commuting subalgebras of the i -th copy of $\mathfrak{so}(4)$.

Substituting this back into the block-diagonal matrix H , we can decompose H into two distinct block-diagonal matrices:

$$H = H_A + H_B,$$

where

$$H_A = \text{diag}(A_1, A_2, \dots, A_k) \quad \text{and} \quad H_B = \text{diag}(B_1, B_2, \dots, B_k).$$

The matrix H_A aggregates all the left-isoclinic components, while H_B aggregates all the right-isoclinic components.

Crucially, these two matrices commute, $[H_A, H_B] = 0$. This is because the commutator of block-diagonal matrices is the block-diagonal matrix of the commutators of their corresponding blocks:

$$[H_A, H_B] = \text{diag}([A_1, B_1], [A_2, B_2], \dots, [A_k, B_k]).$$

As established earlier, $[A_i, B_i] = 0$ for all i , so every block in the resulting matrix is a zero matrix.

This commutativity allows for the final factorization of the exponential map for the entire block-diagonal rotation in $\mathbf{SO}(4k)$:

$$R = \exp(H) = \exp(H_A + H_B) = \exp(H_A) \exp(H_B).$$

The resulting rotation R is the product of two commuting block-diagonal rotations, $R_A = \exp(H_A)$ and $R_B = \exp(H_B)$. Each of these can be computed efficiently block by block using the closed-form Euler-like formula derived previously:

$$\begin{aligned} R_A &= \text{diag}(\exp(A_1), \dots, \exp(A_k)) = \text{diag}(\cos(\theta_{1,i})I + \sin(\theta_{1,i})J_{A_i})_{i=1}^k, \\ R_B &= \text{diag}(\exp(B_1), \dots, \exp(B_k)) = \text{diag}(\cos(\theta_{2,i})I + \sin(\theta_{2,i})J_{B_i})_{i=1}^k. \end{aligned}$$

This framework effectively reduces the complex problem of parameterizing a $4k \times 4k$ rotation within this subgroup to the management of $2k$ independent angles and $2k$ independent 3D axes, offering a computationally tractable and structurally elegant solution.

To apply this machinery in a practical context, such as modeling sequential data where each block corresponds to a specific position, we can introduce a more structured parameterization. Instead of learning independent angles for each position, we can define the rotation for a given position as a function of its index. This enforces a consistent geometric relationship across the sequence.

We introduce global base rotation angles θ_A and θ_B for the two types of isoclinic rotations. The rotation matrices corresponding to positions m and n are then respectively defined as:

$$R(\theta_A, \theta_B, m) = \exp(m\theta_A J_A) \exp(m\theta_B J_B) \quad \text{and} \quad R(\theta_A, \theta_B, n) = \exp(n\theta_A J_A) \exp(n\theta_B J_B).$$

The interaction between two positions m and n is captured by the relative transformation:

$$R(\theta_A, \theta_B, m) R(\theta_A, \theta_B, n)^{-1}.$$

For a single generator, e.g., J_A , the relative transformation simplifies to:

$$\exp(m\theta J_A) \exp(n\theta J_A)^{-1} = \exp((m-n)\theta J_A) = \cos((m-n)\theta)I + \sin((m-n)\theta)J_A.$$

An identical relation holds for the matrix J_B . Since the Lie bracket $[J_A, J_B] = 0$, their exponentials commute, allowing us to write:

$$R(\theta_A, \theta_B, m)R(\theta_A, \theta_B, n)^{-1} = \exp((m-n)\theta_A J_A) \exp((m-n)\theta_B J_B).$$

When the feature dimension D is a multiple of $4k$, we can apply this method to perform rotations in each decoupled 4D subspace. For a position i , we define the transformation matrix as:

$$\mathbf{T}_i = s_i^{-1} R(\theta_A, \theta_B, i) = s_i^{-1} \exp(i\theta_A J_A) \exp(i\theta_B J_B).$$

The interaction between two positions m and n corresponds to the following matrix:

$$\begin{aligned} \mathbf{T}_m \mathbf{T}_n^{-1} &= s_m^{-1} R(\theta_A, \theta_B, m) s_n R(\theta_A, \theta_B, n)^{-1} \\ &= \frac{s_n}{s_m} \exp((m-n)\theta_A J_A) \exp((m-n)\theta_B J_B). \end{aligned}$$

2D PaTE-SO(4)

Notably, this approach is applicable not only to 1D token sequences, as in language models, but also to 2D sequences of image patches. We can associate $J_A \in \mathfrak{h}_1$ with the x -axis and $J_B \in \mathfrak{h}_2$ with the y -axis:

$$\begin{aligned} R(\theta_A, \theta_B, (x_1, y_1)) &= \exp(x_1\theta_A J_A) \exp(y_1\theta_B J_B), \\ R(\theta_A, \theta_B, (x_2, y_2)) &= \exp(x_2\theta_A J_A) \exp(y_2\theta_B J_B). \end{aligned}$$

For two patches located at (x_1, y_1) and (x_2, y_2) , the relative transformation is:

$$\begin{aligned} \mathbf{T}_{(x_1, y_1)} \mathbf{T}_{(x_2, y_2)}^{-1} &= f(x_1, y_1)^{-1} R(\theta_A, \theta_B, (x_1, y_1)) f(x_2, y_2) R(\theta_A, \theta_B, (x_2, y_2))^{-1} \\ &= \frac{f(x_2, y_2)}{f(x_1, y_1)} \exp((x_1 - x_2)\theta_A J_A) \exp((y_1 - y_2)\theta_B J_B). \end{aligned}$$

If we define $\mathbf{M}_{(x_1, y_1)} = f(x_1, y_1)^2 \mathbf{I}$, then the interaction term can be expressed as:

$$\begin{aligned} \mathbf{q}_m^\top \mathbf{M}_m \mathbf{T}_m \mathbf{T}_n^{-1} \mathbf{k}_n &= f(x_1, y_1) f(x_2, y_2) \mathbf{q}_m^\top \exp((x_1 - x_2)\theta_A J_A) \exp((y_1 - y_2)\theta_B J_B) \mathbf{k}_n \\ &= \langle \mathbf{T}_m^{-1} \mathbf{q}_m, \mathbf{T}_n^{-1} \mathbf{k}_n \rangle, \end{aligned}$$

where \mathbf{m} and \mathbf{n} denote 2D positions (x_1, y_1) and (x_2, y_2) for brevity in the expression. The final equation provides a concrete instantiation of our geometric framework for 2D data. The relative transformation is a composition of two orthogonal transformations operating in distinct, commuting subspaces, perfectly encoding the displacement along each spatial axis. This formulation is inherently isotropic, treating the x and y dimensions symmetrically, yet allows for learned anisotropic modulation through the scaling factors s_x and s_y . Ultimately, this method yields a holistic representation of 2D relative positions, standing in contrast to methods that treat spatial dimensions as separate or unstructured features. The unique algebraic structure of $\mathfrak{so}(4)$, specifically its decomposition into two commuting subalgebras, finds a natural correspondence with the geometry of the 2D plane, resulting in a computationally elegant and theoretically robust representation of spatial relationships.

2.5 Inducing Structure on the Trivial Value Bundle

The formalization of value vectors as sections of a trivial bundle, $\mathcal{M} \times \mathbb{R}^{D_v}$, is not merely a descriptive choice; it is a generative one. It provides a principled foundation for introducing more sophisticated, structured operations beyond simple weighted averaging. We explore three such extensions that leverage the fiber bundle structure to enhance the expressive power of the attention mechanism.

Dynamic Fiber Gating

The standard attention mechanism employs a scalar weight, $a_{m,i}$, which uniformly scales all channels of a value vector \mathbf{v}_i . This raises a natural question: should the query \mathbf{q}_m only determine how much information to retrieve from position i , or should it also influence what kind of information is retrieved?

To address this, we introduce a dynamic fiber gating mechanism. We define a learnable gating function, g , that is conditioned on the query vector and acts directly on the value fiber \mathbb{R}^{D_v} . This function maps the query's tangent space to a gating vector in the value space:

$$g : T_{\mathbf{p}_m} \mathcal{M} \rightarrow \mathbb{R}^{D_v}.$$

The aggregation of values is then modulated by this gate, allowing for content-addressable channel selection:

$$\mathbf{o}_m = \sum_i a_{m,i} (g(\mathbf{q}_m) \odot \mathbf{v}_i),$$

where \odot denotes the element-wise product. This mechanism empowers the model to dynamically select and emphasize the most relevant feature channels from a value vector, conditioned on the specific query.

Local Symmetry via Group Action

The trivial bundle construction assumes that value vectors can be directly aggregated. However, for data with inherent geometric properties, it may be beneficial to apply a position-dependent transformation to "align" features before aggregation.

This can be formalized by introducing a group action on the value fiber. Let G be a Lie group acting on \mathbb{R}^{D_v} , such as the special orthogonal group $\mathbf{SO}(D_v)$. We can then learn a mapping, h , from the base manifold to the group itself:

$$h : \mathcal{M} \rightarrow G.$$

The value aggregation is then modified to incorporate these local symmetry transformations:

$$\mathbf{o}_m = \sum_i a_{m,i} (h(\mathbf{p}_i) \cdot \mathbf{v}_i),$$

where $h(\mathbf{p}_i) \cdot \mathbf{v}_i$ represents the action of the group element $h(\mathbf{p}_i)$ (e.g., a rotation matrix) on the vector \mathbf{v}_i . This introduces a powerful inductive bias, often referred to as a local gauge symmetry, allowing the model to learn position-aware feature adaptations.

Connections on the Value Bundle

Our initial assumption of a trivial bundle implies that the "rules" for aggregating values are globally uniform and position-agnostic. We can challenge this assumption by introducing a new, learnable connection on the value bundle.

A connection defines a notion of parallel transport specific to the bundle it is on. Let us denote this new value connection as \mathcal{C} , with its corresponding parallel transport operator $\mathcal{C}_{i \rightarrow m}$. Crucially, this connection is independent of the Riemannian connection on the tangent bundle used for Q/K interactions. The final aggregation step then becomes:

$$\mathbf{o}_m = \sum_i a_{m,i} \mathcal{C}_{i \rightarrow m}(\mathbf{v}_i).$$

This establishes a dual-geometry framework:

- 1) A Riemannian geometry on the tangent bundle governs the Q/K interactions, determining **where to attend**.
- 2) A gauge-like geometry, defined by the learned value connection \mathcal{C} , governs the V aggregation, determining **how to integrate the attended information**.

This provides maximal flexibility, allowing the model to learn, for instance, that information from distant tokens should be transformed (e.g., blurred or down-weighted) differently than information from nearby tokens during the final value aggregation.

A Concrete Realization: The Locality Focusing Mechanism

While the concepts of dynamic gating, group actions, and fully learned connections represent powerful avenues for future research, we now introduce a practical and highly effective mechanism that realizes the core principle of a structured value bundle with minimal overhead. This approach can be understood as a specific instantiation of a predefined connection on the value bundle. Instead of a complex learnable operator, this connection is simplified to a position-dependent scalar modulation, designed explicitly to enforce a local inductive bias. We term this mechanism Locality Focusing.

Unlike CNNs, which are endowed with locality and translational equivariance, vanilla transformers are data-hungry due to their minimal inductive biases. This flexibility makes them powerful on large, diverse datasets but can be a limitation on limited data, where domain-specific priors are crucial for generalization. Our Locality Focusing mechanism directly addresses this by introducing an explicit neighborhood bias, attenuating the influence of remote values during aggregation.

Consistent with the trivial bundle structure that places value vectors in a global Euclidean space \mathbb{R}^D , this modulation is performed directly on the values prior to their final weighting. While attention scores implicitly reflect semantic relevance, Locality Focusing enforces a strong spatial bias. Specifically, for a given query position m , we modulate each value vector \mathbf{v}_i by a position-relative decay factor, $\lambda_{m,i}$. This factor is designed to be a monotonic function of the distance between positions m and i . The final output vector for position m is then computed as the weighted sum of these modulated values, where $s_{m,i}$ are the softmax-normalized attention scores:

$$\mathbf{o}_m = \sum_i s_{m,i} (\lambda_{m,i} \mathbf{v}_i).$$

This approach effectively disentangles the "what" (semantic relevance from attention) from the "where" (spatial locality from the λ factors), providing a more robust and controllable inductive bias. In matrix form, the output for a single query \mathbf{q}_m is:

$$\mathbf{o}_m = \text{Attn}(\mathbf{q}_m, \mathbf{K}, \mathbf{\Lambda}_m, \mathbf{V}) = \mathbf{C}_m (\mathbf{\Lambda}_m \mathbf{V}), \quad (14)$$

where $\mathbf{C}_m \in \mathbb{R}^{1 \times N}$, $\mathbf{K}, \mathbf{V} \in \mathbb{R}^{N \times D}$, and $\mathbf{\Lambda}_m \in \mathbb{R}^{N \times N}$ is a diagonal matrix containing the factors $\{\lambda_{m,i}\}_{i=1}^N$. This expands to:

$$\begin{aligned} \mathbf{o}_m &= [C_{m,1} \quad C_{m,2} \quad \cdots \quad C_{m,N}] \text{diag}(\lambda_{m,1}, \lambda_{m,2}, \cdots, \lambda_{m,N}) \begin{bmatrix} \mathbf{v}_1 \\ \mathbf{v}_2 \\ \vdots \\ \mathbf{v}_N \end{bmatrix} \\ &= [C_{m,1} \quad C_{m,2} \quad \cdots \quad C_{m,N}] \begin{bmatrix} \lambda_{m,1} \mathbf{v}_1 \\ \lambda_{m,2} \mathbf{v}_2 \\ \vdots \\ \lambda_{m,N} \mathbf{v}_N \end{bmatrix}. \end{aligned} \quad (15)$$

This mechanism, while presented here for 2D image data, is equally applicable to n-dimensional sequences. Its formulation is strongly reminiscent of the bilateral filter from image processing, which smooths images while preserving edges:

$$\mathbf{o}_m = \sum_{n=1}^N \underbrace{G_s(\mathbf{q}_m, \mathbf{k}_n)}_{\text{Intensity Similarity}} \underbrace{G_\sigma(\mathbf{d}_m, \mathbf{d}_n)}_{\text{Spatial Proximity}} \mathbf{v}_n, \quad (16)$$

Here, the attention term $G_s(\cdot, \cdot)$ plays the role of the intensity/range kernel, measuring similarity in feature space, while our attenuation factor $G_\sigma(\cdot, \cdot)$ acts as the spatial/domain kernel. A common choice for G_σ is a Gaussian function of the distance between positions \mathbf{d}_m and \mathbf{d}_n , $G_\sigma(\mathbf{x}, \mathbf{y}) = e^{-\frac{\|\mathbf{x}-\mathbf{y}\|_2^2}{2\sigma^2}}$, where \mathbf{A} and σ can be learnable.

For efficient implementation across all tokens, the attenuation factors for all query positions can be collected into a single $N \times N$ matrix $\mathbf{\Omega}$, where $\Omega_{m,i} = \lambda_{m,i}$. The full attention output is then computed as:

$$\mathbf{O} = (\mathbf{C} \odot \mathbf{\Omega})\mathbf{V} = \left(\begin{bmatrix} C_{1,1} & C_{1,2} & \cdots & C_{1,N} \\ C_{2,1} & C_{2,2} & \cdots & C_{2,N} \\ \vdots & \vdots & \ddots & \vdots \\ C_{N,1} & C_{N,2} & \cdots & C_{N,N} \end{bmatrix} \odot \begin{bmatrix} \lambda_{1,1} & \lambda_{1,2} & \cdots & \lambda_{1,N} \\ \lambda_{2,1} & \lambda_{2,2} & \cdots & \lambda_{2,N} \\ \vdots & \vdots & \ddots & \vdots \\ \lambda_{N,1} & \lambda_{N,2} & \cdots & \lambda_{N,N} \end{bmatrix} \right) \cdot \mathbf{V}. \quad (17)$$

This simple mechanism significantly improves the capacity of transformers to learn the inductive bias of locality, especially on smaller datasets. As our experiments reveal, incorporating such an explicit local focusing mechanism substantially improves the performance of transformers in visual tasks.

3 Experiments

This study primarily focuses on the visual domain and, consequently, evaluates the performance of RiemnnFormer on image classification tasks for small datasets.

Image data inherently possesses a 2D structure defined by two spatial axes. While standard approaches often flatten patches into a 1D sequence or address these dimensions jointly [14], our PaTE-SO(4) framework offers a mathematically natural correspondence. The algebraic decomposition of SO(4) yields two commuting sets of rotational generators (left- and right-isoclinic rotations). This dual-axis structure aligns perfectly with the Cartesian geometry of images, allowing us to explicitly and simultaneously encode the height and width dimensions within the same unified representation.

We define the Riemannian metric at a patch position (x, y) as $\mathbf{M}_{(x,y)} = f(x, y)^2 \mathbf{I}$. Adopting PaTE-SO(4) as a representative instantiation, the interaction between two tokens located at different positions can be expressed as:

$$\langle \mathbf{T}_{(x_1,y_1)}^{-1} \mathbf{q}_{(x_1,y_1)}, \mathbf{T}_{(x_2,y_2)}^{-1} \mathbf{k}_{(x_2,y_2)} \rangle = f(x_1, y_1) f(x_2, y_2) \mathbf{q}_{(x_1,y_1)}^\top \exp((x_1 - x_2) \theta_A J_A) \exp((y_1 - y_2) \theta_B J_B) \mathbf{k}_{(x_2,y_2)}$$

where $\mathbf{T}_{(x,y)} = f(x, y)^{-1} R(\theta_A, \theta_B, (x, y))$ encapsulates both rotation and scaling. Then we decouple the scaling component from the Softmax to form our attention module $\text{RieAttn} = \left(\mathbf{L}\mathbf{L}^\top \odot \text{Softmax} \left(\frac{\mathbf{R}[\mathbf{Q}]\mathbf{R}[\mathbf{K}]^\top}{\sqrt{d_k}} \right) \right) \mathbf{V}$.

To empirically validate the efficacy of this geometrically principled mechanism, particularly in capturing intrinsic spatial structures, we integrate it into a practical vision backbone. The proposed modules undergo training and evaluation on the CIFAR-10 and CIFAR-100 datasets, employing a lightweight Vision Transformer (ViT) architecture. Specifically, these modules leverage the compact yet efficient structure of the ViT model to process the image classification tasks inherent to these benchmark datasets. All experiments were implemented on an NVIDIA RTX 4090 GPU with PyTorch 2.7. The training procedure is conducted over 100 epochs with a batch size of 128, utilizing the AdamW optimizer configured with its default hyperparameters.

In our experimental evaluation, we implement and compare both PaTE-SO(2) and PaTE-SO(4) variants. For both formulations, the rotation operations rely on a specific angle configuration across different subspaces. We define an angle schedule function that maps a subspace index to its corresponding rotation angle. Empirically, we observed that a straightforward harmonic schedule yields favorable results: $f(t) : t \mapsto t\theta$, $t \in \{1, 2, \dots, K\}$, where θ is a learnable base frequency and t denotes the subspace index.

Furthermore, for the PaTE-SO(4) instantiation, the geometric configuration extends beyond mere angles to the orientation of the rotation axes (specifically, the axes for the left and right isoclinic rotations). To investigate the trade-off between geometric flexibility and parameter efficiency, we evaluate two distinct axis strategies: independent axes, where each subspace learns its own unique rotation axis, and shared axes, where a single global axis orientation is applied across all subspaces.

The current work is primarily dedicated to further exploring the potential of transformer-based models in visual tasks, and thus, it mainly compares with ViT architectures. The architecture of our ultra-lightweight vision transformer comprises only 4 attention heads, 6 transformer layers, and decomposes images into 64 patches, each of 4×4 pixels. The results from the experiments are compiled in Table 1. CIFAR-10 and CIFAR-100 are both widely used datasets in the field of computer vision and machine learning, specifically for image classification tasks. It is evident that our method exhibits greater enhancement over traditional positional encodings on datasets with fewer images per category (CIFAR-100). CIFAR-100 is used for more rigorous testing of models, particularly to evaluate their performance on a larger number of classes and to understand how well they can generalize across a broader range of categories.

Table 1 presents the preliminary experimental results of our proposed algorithms on the CIFAR-10 and CIFAR-100 datasets. For clarity, the abbreviations used in the table are defined as follows: Rot denotes the rotational component;

Table 1: Results of the Proposed Models on Small Datasets in Image Classification Benchmarks.

Models Datasets	PaTESO(2)			PaTESO(4)				
	Rot	Rot+Scl	Rot+Scl+LF	Rot	Rot+Scl	Rot+Scl(SA)	Rot+Scl+LF	Rot+Scl+LF(SA)
CIFAR-10	82.11	83.68	85.71	84.75	85.44	85.32	85.61	86.10
CIFAR-100	53.49	53.81	57.49	55.43	55.39	57.68	58.75	58.98

Scl represents the Riemannian metric scaling; LF refers to the Locality Focusing Mechanism; and SA indicates the Shared Axis strategy within the PaTESO(4) framework, where the rotation axes are shared across all subspaces.

A comparative analysis of the tabulated data reveals several key insights into the proposed framework. First, PaTESO(4) consistently outperforms PaTESO(2) across both datasets and configurations (e.g., increasing from 82.11% to 84.75% in the base 'Rot' setting on CIFAR-10), suggesting that the higher-dimensional rotational structure of SO(4) captures spatial relationships more effectively than SO(2). Second, the integration of Riemannian metric scaling (Scl) yields observable gains over the pure rotation baseline in most cases, validating the hypothesis that modulating the geometry based on content or position enhances representation. Third, the Locality Focusing (LF) mechanism provides a significant performance boost (e.g., reaching 85.71% in PaTESO(2)), highlighting the importance of inductive biases for local neighborhood attention in visual tasks. Finally, the combination of all components yields the highest accuracy, with PaTESO(4) using the Shared Axis (SA) strategy achieving the best overall results (86.10% on CIFAR-10 and 58.98% on CIFAR-100).

It is important to note that the primary objective of these experiments is to evaluate the relative efficacy of different geometric schemes rather than to chase state-of-the-art absolute performance. Consequently, we employed a relatively small network architecture and a limited number of training iterations. For the metric scaling (Scl), we adopted a dynamic approach where the scale is determined by the embeddings using the simple projection scheme defined in Eq. (10). Regarding PaTESO(4), we observed that the Shared Axis (SA) variant appears to perform slightly better than the independent axis configuration under the current angle strategy. We hypothesize that this may be due to the regularization effect of sharing parameters, which is particularly beneficial given the current model scale and parameter constraints. Further investigations on larger datasets and deeper networks are required to fully validate the scalability of the independent axis strategy.

4 Conclusion

WE present RiemannFormer, a framework that reimagines the Transformer through the lens of differential geometry. We assume that the tokens reside in a curved space, and their latent representations are governed by parallel transport and Riemannian metrics. Our approach utilizes predefined Lie group structures to capture spatial dependencies efficiently, removing the reliance on traditional positional embeddings. A key contribution is the Riemannian Attention Mechanism, which strategically decouples metric scaling from softmax normalization. This design allows us to implement a dynamic scaling strategy where the embedding content itself dictates the local geometry — akin to mass curving spacetime. This mechanism not only serves as an effective locality bias by attenuating remote interactions but also provides a content-aware gating capability.

The framework outlined in this paper has been demonstrated to effectively improve the performance of transformers by conducting experiments on the CIFAR-10 and CIFAR-100 datasets. Our experimental results confirm that properly modeling this intrinsic geometry yields significant performance gains, particularly in visual tasks. The current implementation in this paper serves as a preliminary validation of our insights, and further evaluation experiments involving more visual models and large language models will be conducted sequentially.

References

- [1] Ashish Vaswani, Noam Shazeer, Niki Parmar, Jakob Uszkoreit, Llion Jones, Aidan N Gomez, Łukasz Kaiser, and Illia Polosukhin. Attention is all you need. In I. Guyon, U. V. Luxburg, S. Bengio, H. Wallach, R. Fergus, S. Vishwanathan, and R. Garnett, editors, *Advances in Neural Information Processing Systems*, volume 30. Curran Associates, Inc., 2017. 1, 2

- [2] Jacob Devlin, Ming-Wei Chang, Kenton Lee, and Kristina Toutanova. BERT: pre-training of deep bidirectional transformers for language understanding. In *Proceedings of the 2019 Conference of the North American Chapter of the Association for Computational Linguistics: Human Language Technologies, NAACL-HLT 2019, Minneapolis, MN, USA, June 2-7, 2019, Volume 1 (Long and Short Papers)*, pages 4171–4186. Association for Computational Linguistics, 2019. [2](#)
- [3] Zihang Dai, Z. Yang, Yiming Yang, J. Carbonell, Quoc V. Le, and R. Salakhutdinov. Transformer-xl: Attentive language models beyond a fixed-length context. In *ACL*, 2019. [2](#)
- [4] Colin Raffel, Noam Shazeer, Adam Roberts, Katherine Lee, Sharan Narang, Michael Matena, Yanqi Zhou, Wei Li, and Peter J. Liu. Exploring the limits of transfer learning with a unified text-to-text transformer. *Journal of Machine Learning Research*, 21(140):1–67, 2020. [2](#)
- [5] Guolin Ke, Di He, and Tie-Yan Liu. Rethinking positional encoding in language pre-training. In *9th International Conference on Learning Representations, ICLR 2021, Virtual Event, Austria, May 3-7, 2021*. OpenReview.net, 2021. [2](#)
- [6] Jianlin Su, Murtadha Ahmed, Yu Lu, Shengfeng Pan, Wen Bo, and Yunfeng Liu. Roformer: Enhanced transformer with rotary position embedding. *Neurocomputing*, 568, 2024. [2](#)
- [7] Yutao Sun, Li Dong, Barun Patra, Shuming Ma, Shaohan Huang, Alon Benhaim, Vishrav Chaudhary, Xia Song, and Furu Wei. A length-extrapolatable transformer. In Anna Rogers, Jordan Boyd-Graber, and Naoaki Okazaki, editors, *Proceedings of the 61st Annual Meeting of the Association for Computational Linguistics (Volume 1: Long Papers)*, pages 14590–14604, Toronto, Canada, 2023. [2](#)
- [8] Ofir Press, Noah Smith, and Mike Lewis. Train short, test long: Attention with linear biases enables input length extrapolation. In *International Conference on Learning Representations*, 2022. [2](#)
- [9] Chuanyang Zheng, Yihang Gao, Han Shi, Minbin Huang, Jingyao Li, Jing Xiong, Xiaozhe Ren, Michael Ng, Xin Jiang, Zhenguo Li, and Yu Li. Dape: Data-adaptive positional encoding for length extrapolation, 2024. [2](#)
- [10] Olga Golovneva, Tianlu Wang, Jason Weston, and Sainbayar Sukhbaatar. Contextual position encoding: Learning to count what’s important, 2024. [2](#)
- [11] Alexey Dosovitskiy, Lucas Beyer, Alexander Kolesnikov, Dirk Weissenborn, Xiaohua Zhai, Thomas Unterthiner, Mostafa Dehghani, Matthias Minderer, Georg Heigold, Sylvain Gelly, Jakob Uszkoreit, and Neil Houlsby. An image is worth 16x16 words: Transformers for image recognition at scale. In *9th International Conference on Learning Representations, ICLR 2021, Virtual Event, Austria, May 3-7, 2021*, 2021. [2](#)
- [12] Hugo Touvron, Matthieu Cord, Matthijs Douze, Francisco Massa, Alexandre Sablayrolles, and Hervé Jégou. Training data-efficient image transformers & distillation through attention. In *ICML*, pages 10347–10357, 2021. [2](#)
- [13] Nicolas Carion, Francisco Massa, Gabriel Synnaeve, Nicolas Usunier, Alexander Kirillov, and Sergey Zagoruyko. End-to-end object detection with transformers. In Andrea Vedaldi, Horst Bischof, Thomas Brox, and Jan-Michael Frahm, editors, *Computer Vision – ECCV 2020*, pages 213–229, Cham, 2020. Springer International Publishing. [2](#)
- [14] Byeongho Heo, Song Park, Dongyoon Han, and Sangdoon Yun. Rotary position embedding for vision transformer. In *European Conference on Computer Vision (ECCV)*, 2024. [2](#), [16](#)
- [15] Xiangxiang Chu, Zhi Tian, Bo Zhang, Xinlong Wang, and Chunhua Shen. Conditional positional encodings for vision transformers. In *ICLR 2023*, 2023. [2](#)